Brain-derived estrogens facilitate male-typical behaviors by potentiating androgen receptor signaling in medaka

Yuji Nishiike[1], Shizuku Maki[1], Daichi Miyazoe[1], Kiyoshi Nakasone[1], Yasuhiro Kamei[2], Takeshi Todo[3], Tomoko Ishikawa-Fujiwara[3], Kaoru Ohno[4], Takeshi Usami[4], Yoshitaka Nagahama[4], and Kataaki Okubo[1,*]

[1]Department of Aquatic Bioscience, Graduate School of Agricultural and Life Sciences, The University of Tokyo, Bunkyo, Tokyo 113-8657, Japan; [2]Optics and Bioimaging Facility, Trans-Scale Biology Center, National Institute for Basic Biology, Okazaki, Aichi 444-8585, Japan; [3]Department of Genome Biology, Graduate School of Medicine, Osaka University, Suita, Osaka 565-0871, Japan; [4]Division of Reproductive Biology, National Institute for Basic Biology, Okazaki, Aichi 444-8585, Japan

***For correspondence:** a-okubo@g.ecc.u-tokyo.ac.jp

Abstract

In rodents, estrogens aromatized from androgens in the brain are essential for the development of male-typical behaviors. In many other vertebrates including humans and teleost fish, however, androgens facilitate these behaviors directly via the androgen receptor without aromatization into estrogens. Here we report that mutagenesis-derived male medaka fish lacking Cyp19a1b (a subtype of aromatase predominantly expressed in the brain) exhibit severely impaired male-typical mating and aggression, despite elevated brain androgen levels. These phenotypes can be rescued by estrogen administration, indicating that brain-derived estrogens are pivotal for male-typical behaviors even in teleosts. Our results further suggest that these estrogens facilitate male-typical behaviors by potentiating androgen action in the brain via the direct stimulation of androgen receptor transcription. Taken together, these findings reveal a previously unappreciated mode of action of brain-derived estrogens in shaping male-typical behaviors.

Keywords: aggression; androgen receptor; aromatase; mating; brain-derived estrogens

Introduction

Male and female animals exhibit differences in many innate behaviors, such as mating and aggression (Zilkha et al., 2021). In vertebrates, these differences are driven primarily by the influence of sex steroid hormones, including estrogens and androgens. Extensive research in rodents has established that estrogens, traditionally considered "female" hormones, are critical for the development of male-typical behaviors (Ogawa et al., 2020; Tsukahara et al., 2020; McCarthy, 2023). Specifically, androgens secreted by the testis, both perinatally and in adulthood, are converted to estrogens in the brain by the enzyme aromatase. These estrogens then act through ESR1, a subtype of the estrogen receptor (ESR), to elicit male-typical behaviors (Ogawa et al., 2020; Tsukahara et al., 2020; McCarthy, 2023). This process, originally referred to as the "aromatization hypothesis", is now widely acknowledged; however, the mechanisms through which brain-derived estrogens affect male-typical behavior, including the identity of their downstream targets, remain largely elusive (McCarthy et al., 2017; McCarthy, 2023).

More importantly, the aromatization hypothesis seems to apply to only a limited number of species besides rodents (e.g., some birds such as zebra finches) (Balthazart, 2019). In other species such as humans, other primates, and teleost fish, testicular androgens facilitate male-typical behaviors directly through the androgen receptor (AR) without aromatization (Thornton et al., 2009; Bakker, 2022; Okubo et al., 2022). In primates, the hypothalamic aromatization of androgens to estrogens plays a central role in female gametogenesis (Terasawa, 2018) but is not essential for male behaviors (Thornton et al., 2009; Bakker, 2022). Notably, in teleosts, 11-ketotestosterone (11KT), which cannot be aromatized to estrogens, is the primary testicular androgen, and exogenous 11KT effectively induces male-typical courtship and aggression even in females (Nishiike et al., 2021; Okubo et al., 2022; Kawabata-Sakata et al., 2024). Therefore, it is generally assumed that, in teleosts, androgens are largely responsible for male-typical behaviors, while estrogens are dispensable for these behaviors. This is consistent with recent observations in a few teleost species that genetic ablation of AR severely impairs male-typical behaviors (Yong et al., 2017; Alward et al., 2020; Ogino et al., 2023; Nishiike and Okubo, 2024) and with findings in medaka fish (*Oryzias latipes*) that estrogens act through the ESR subtype Esr2b to prevent females from engaging in male-typical courtship (Nishiike et al., 2021).

Interestingly, despite these findings, adult teleost brains have extremely high levels of aromatase activity (100–1000 times higher than in rodent brains), resulting in large amounts of brain estrogens even in males (Diotel et al., 2018). In teleost brains, including those of medaka, aromatase is exclusively localized in radial glial cells, in contrast to its neuronal localization in rodent brains (Forlano et al., 2001; Diotel et al., 2010; Takeuchi and Okubo, 2013). These observations suggest that brain-derived estrogens have a vital, but as yet undetermined, role in male teleosts. It is worth mentioning that systemic administration of estrogens and an aromatase inhibitor increased and decreased male aggression, respectively, in several teleost species, potentially reflecting the behavioral effects of brain-derived estrogens (Hallgren et al., 2006; O'Connell and Hofmann, 2012; Huffman et al., 2013; Jalabert et al.,

2015). Most teleost species have two distinct genes encoding aromatase, *cyp19a1a* and *cyp19a1b*, due to a whole-genome duplication that occurred early in teleost evolution (Diotel et al., 2018; Nagahama et al., 2021). These genes have undergone subfunctionalization through the partitioning of tissue-specific expression patterns: *cyp19a1a* is expressed predominantly in the gonad, whereas *cyp19a1b* is expressed in the brain (Diotel et al., 2018; Nagahama et al., 2021). In medaka, *cyp19a1b* is also expressed in the gonads, but only at a level tens to hundreds of times lower than in the brain and substantially lower than that of *cyp19a1a* (Okubo et al., 2011; Nakamoto et al., 2018).

In the present study, we generated *cyp19a1b*-deficient medaka, in which estrogen synthesis in the brain is selectively impaired while that in the gonads remains intact, in order to investigate the impact of brain-derived estrogens on male behaviors. Remarkably, the fish showed severely impaired male-typical behaviors, thus revealing the marked behavioral effects of these estrogens. Our results further suggest that these effects are mediated by potentiating androgen signaling in behaviorally relevant brain regions.

Results

cyp19a1b-deficient males exhibit severely impaired male-typical mating and aggressive behaviors

We generated a *cyp19a1b*-deficient medaka line from a mutant founder carrying a nonsense mutation in exon 4 of *cyp19a1b* that was identified through screening of the medaka TILLING (targeting-induced local lesions in genomes) library (Taniguchi et al., 2006) (Figure 1—figure supplement 1A and B). Loss of *cyp19a1b* function in these fish was verified by measuring brain and peripheral levels of sex steroids in males. As expected, brain estradiol-17β (E2) in homozygous mutants (*cyp19a1b*$^{-/-}$) was significantly reduced to 16% of the levels in wild-type (*cyp19a1b*$^{+/+}$) siblings (P = 0.0037) (Figure 1A). Brain E2 in heterozygotes (*cyp19a1b*$^{+/-}$) was also reduced to 45% of wild-type levels (P = 0.0284) (Figure 1A), indicating a dosage effect of the *cyp19a1b* mutation. In contrast, peripheral E2 levels were unaltered in *cyp19a1b*$^{-/-}$ males (Figure 1B), consistent with the expected functioning of Cyp19a1b primarily in the brain. Strikingly, brain testosterone levels, as opposed to E2, increased 2.2-fold in *cyp19a1b*$^{-/-}$ males relative to wild-type siblings (P = 0.0006) (Figure 1A). Similarly, brain 11KT levels increased 6.2-fold (P = 0.0007) (Figure 1A). These results indicate that *cyp19a1b*-deficient males have reduced estrogen coupled with elevated androgen levels in the brain, confirming the loss of *cyp19a1b* function. They also suggest that the majority of estrogens in the male brain are synthesized locally in the brain. Peripheral 11KT levels also increased 3.7-fold in *cyp19a1b*$^{-/-}$ males (P = 0.0789) (Figure 1B), indicating peripheral influence in addition to central effects.

Loss of *cyp19a1b* function was further confirmed by measuring *cyp19a1b* transcript levels in the brain and by predicting the three-dimensional structure of the mutant protein. Real-time PCR revealed that transcript levels were reduced by half in *cyp19a1b*$^{+/-}$ males and were nearly undetectable in *cyp19a1b*$^{-/-}$ males, presumably as a result of nonsense-mediated mRNA decay (Lindeboom et al., 2019) (Figure 1C). The wild-type protein, modeled by AlphaFold 3, exhibited a typical cytochrome P450 fold, including the membrane helix, aromatic region, and heme-binding loop, all arranged in the expected configuration (Figure 1—figure supplement 1C). The mutant protein, in contrast, was severely truncated, retaining only the membrane helix (Figure 1—figure supplement 1C). The absence of essential domains strongly indicates that the allele encodes a non-functional Cyp19a1b protein. Together, transcript and structural analyses consistently demonstrate that the mutation generated in this study causes a complete loss of *cyp19a1b* function.

Next, we investigated the mating behavior of *cyp19a1b*-deficient males (Figure 1D). The mating behavior of medaka follows a stereotypical sequence. It begins with the male approaching and closely following the female (following). The male then performs a courtship display, rapidly swimming in a circular pattern in front of the female. If the female is receptive, the male grasps her with his fins (wrapping), culminating in the simultaneous release of eggs and sperm (spawning) (Nishiike and Okubo, 2024). Because 11KT, the primary driver of male-typical behaviors in teleosts, was increased in *cyp19a1b*-deficient males, we predicted that these fish would engage more actively in mating.

119 Nevertheless, *cyp19a1b*$^{-/-}$ males showed significantly longer latencies to initiate wrappings ($P = 0.0033$
120 versus *cyp19a1b*$^{+/+}$, $P = 0.0195$ versus *cyp19a1b*$^{+/-}$) and to spawn ($P = 0.0051$ versus *cyp19a1b*$^{+/+}$, $P =$
121 0.0195 versus *cyp19a1b*$^{+/-}$) (Figure 1E). These results suggest that they are less motivated to mate,
122 though an alternative interpretation that their cognition or sexual preference may be altered cannot be
123 dismissed.

124 However, no significant differences were evident in latencies to initiate followings and courtship
125 displays (Figure 1E); therefore, the possibility that *cyp19a1b*-deficient males are less sexually attractive
126 and less preferred by females could not be ruled out. To ascertain whether *cyp19a1b*-deficient males are
127 indeed less motivated to mate, we further tested their mating behavior using *esr2b*-deficient females,
128 which are unreceptive to male courtship (Nishiike et al., 2021), as stimulus females (Figure 1F); this test
129 eliminates the influence of female receptivity, facilitating an exclusive evaluation of male motivation to
130 mate with females (Nishiike and Okubo, 2024). We found that *cyp19a1b*$^{-/-}$ males showed significantly
131 longer latencies to initiate followings ($P = 0.0129$ versus *cyp19a1b*$^{+/+}$, $P = 0.0060$ versus *cyp19a1b*$^{+/-}$),
132 courtship displays ($P = 0.0003$ versus *cyp19a1b*$^{+/+}$, $P = 0.0006$ versus *cyp19a1b*$^{+/-}$), and wrapping
133 attempts ($P = 0.0009$ versus *cyp19a1b*$^{+/+}$, $P = 0.0282$ versus *cyp19a1b*$^{+/-}$) (Figure 1G). In addition, they
134 exhibited significantly fewer courtship displays ($P < 0.0001$ versus both *cyp19a1b*$^{+/+}$ and *cyp19a1b*$^{+/-}$)
135 and wrapping attempts ($P < 0.0001$ versus both *cyp19a1b*$^{+/+}$ and *cyp19a1b*$^{+/-}$) (Figure 1H). These results
136 thus confirmed that *cyp19a1b*-deficient males are less motivated to mate. In our previous study, we
137 found that *esr2b*-deficient females court females preferentially over males (Nishiike et al., 2021).
138 Consistent with that finding, here we observed that 12 of 15 *cyp19a1b*$^{+/+}$ females received courtship
139 displays from the *esr2b*-deficient female, as compared with only 2 of 15 *cyp19a1b*$^{+/+}$ males ($P = 0.0003$)
140 (Figure 1I). Curiously, we further observed that 8 of 15 *cyp19a1b*$^{-/-}$ males received courtship displays
141 from the *esr2b*-deficient female ($P = 0.0321$ versus *cyp19a1b*$^{+/+}$ males) (Figure 1I). Perhaps *cyp19a1b*$^{-/-}$
142 males are misidentified as females by *esr2b*-deficient females because they are reluctant to court or they
143 exhibit some female-like behavior.

144 Next, we examined the intrasexual aggressive behavior of *cyp19a1b*-deficient males (Figure 1J).
145 The aggressive behavior of teleosts including medaka consists of five types of behavioral acts: chases,
146 fin displays, circles, strikes, and bites (Yamashita et al., 2020). *cyp19a1b*$^{-/-}$ males exhibited all of these
147 aggressive acts less frequently than *cyp19a1b*$^{+/+}$ and/or *cyp19a1b*$^{+/-}$ males, with significant differences
148 observed for chases ($P = 0.0123$ versus *cyp19a1b*$^{+/-}$), fin displays ($P = 0.0214$ versus *cyp19a1b*$^{+/+}$), and
149 bites ($P = 0.0015$ versus *cyp19a1b*$^{+/+}$, $P = 0.0002$ versus *cyp19a1b*$^{+/-}$) (Figure 1K). These observations
150 demonstrate that *cyp19a1b*-deficient males are less aggressive toward other males.

151 In tilapia (*Oreochromis niloticus*), depletion of *cyp19a1b* has been reported to cause male infertility
152 due to efferent duct obstruction (Zhang et al., 2019). If this is also the case in medaka, the observed
153 behavioral defects might be secondary to infertility, possibly due to the perception of impaired sperm
154 release. We therefore investigated the fertilization and hatching success of embryos derived from mating
155 between *cyp19a1b*$^{-/-}$ males and wild-type females. Their fertilization and hatching rates were 88.5% (n
156 = 183) and 93.2% (n = 162), respectively, indicating that *cyp19a1b*-deficient male medaka have normal

157 fertility.
158
159 **Brain-derived estrogens facilitate male-typical behaviors probably by stimulating brain**
160 **AR expression**
161 We considered that the impaired male-typical behaviors of *cyp19a1b*-deficient males might be
162 reasonably attributed to either reduced E2 or increased 11KT in the brain. The latter possibility seemed
163 unlikely because 11KT/AR signaling strongly promotes male-typical behaviors in teleosts (Yong et al.,
164 2017; Alward et al., 2020; Okubo et al., 2022; Ogino et al., 2023; Nishiike and Okubo, 2024); therefore,
165 we tested the former possibility by examining whether E2 treatment would rescue the behavioral
166 phenotypes of *cyp19a1b*-deficient males (Figure 2A). E2 treatment, while having no effect in
167 *cyp19a1b*$^{+/+}$ males (Figure 2B and C), significantly shortened the latency to (P = 0.0005) and increased
168 the number of (P = 0.0006) courtship displays in *cyp19a1b*$^{-/-}$ males (Figure 2D and E). These results
169 suggest that reduced E2 in the brain is the primary cause of the mating defects, highlighting a pivotal
170 role of brain-derived estrogens in male mating behavior. However, caution is warranted, as an indirect
171 peripheral effect of bath-immersed E2 on behavior cannot be ruled out, although this is unlikely given
172 the comparable peripheral E2 levels in *cyp19a1b*-deficient and wild-type males. In contrast to mating,
173 E2 treatment was not effective in restoring aggression in *cyp19a1b*$^{-/-}$ males (Figure 2—figure
174 supplement 1A). It is possible that the treatment protocol used may have failed to replicate the estrogenic
175 milieu necessary to induce aggression in males.
176 We then considered the mechanism by which brain-derived estrogens facilitate male-typical
177 behaviors. Our previous study showed that exogenous E2 upregulates the expression of a subtype of AR,
178 Ara, in the medaka brain (Hiraki et al., 2012; note that Ara was termed Arb in this reference). We
179 therefore hypothesized that brain-derived estrogens may facilitate male-typical behaviors by stimulating
180 Ara expression and thereby potentiating 11KT/Ara signaling in the brain. To test this hypothesis, we
181 first examined *ara* expression in the brain of *cyp19a1b*-deficient males by in situ hybridization analysis.
182 Expression of *ara* was significantly lower in *cyp19a1b*$^{-/-}$ males than in *cyp19a1b*$^{+/+}$ males in several
183 preoptic and hypothalamic nuclei that are activated upon mating and/or attack in males (Nishiike and
184 Okubo, 2024), including the PPa, pPPp, and NVT (P = 0.0134, 0.0372, and 0.0008, respectively) (Figure
185 2F and G, Supplementary file 1 for abbreviations of brain nuclei). We then performed a similar analysis
186 for the other AR subtype, Arb. Expression of *arb* was significantly lower in *cyp19a1b*$^{-/-}$ than in
187 *cyp19a1b*$^{+/+}$ males in other preoptic and hypothalamic nuclei activated upon mating and/or attack
188 (Nishiike and Okubo, 2024), including the PMp, aPPp, and NPT (P = 0.0009, 0.0413, and 0.0021,
189 respectively) (Figure 2H and I).
190 Next, to determine whether these reductions in *ara* and *arb* expression in *cyp19a1b*$^{-/-}$ males were
191 the result of reduced brain E2, we tested whether E2 treatment could restore the expression of the two
192 genes. In situ hybridization revealed significantly increased *ara* and *arb* expression in most brain nuclei
193 of E2-treated *cyp19a1b*$^{-/-}$ males as compared with vehicle-treated *cyp19a1b*$^{-/-}$ males (similar results
194 were obtained in *cyp19a1b*$^{+/+}$ males) (Figure 2J and K, Figure 2—figure supplement 1B and C, Figure

195 2—figure supplement 2), indicating that the decreased *ara* and *arb* expression in *cyp19a1b*$^{-/-}$ males is
196 attributable to reduced E2 levels. Taken together, these results suggest that brain-derived estrogens elicit
197 male-typical behaviors by stimulating *ara* and *arb* expression in behaviorally relevant brain regions.
198

199 **_cyp19a1b_ deficiency impairs behaviorally relevant signaling pathways downstream of**
200 **ARs**

201 We considered that, if our hypothesis that brain-derived estrogens facilitate male-typical behaviors
202 by potentiating androgen/AR signaling is correct, then *cyp19a1b*-deficient males should have impaired
203 activation of behaviorally relevant genes that act downstream of ARs. Two neuropeptide genes, *vt*
204 (encoding vasotocin) and *gal* (encoding galanin), have been implicated in male-typical mating and
205 aggressive behaviors in various vertebrates, including medaka and other teleosts (Yokoi et al., 2015;
206 Tripp et al., 2020; Yamashita et al., 2020; Kawabata-Sakata et al., 2024; Nishiike and Okubo, 2024). In
207 medaka, subsets of neurons in the pNVT and pPMp express *vt* and *gal*, respectively, in an androgen-
208 dependent and hence male-biased manner, and these neurons have been implicated in male-typical
209 behaviors (Kawabata et al., 2012; Yamashita et al., 2020; Kawabata-Sakata et al., 2024). We therefore
210 studied the expression of *vt* and *gal* in the brains of *cyp19a1b*-deficient males.

211 In situ hybridization revealed that, as expected, expression of *vt* in the pNVT of *cyp19a1b*$^{-/-}$ males
212 was significantly reduced to 18% as compared with *cyp19a1b*$^{+/+}$ males ($P = 0.0040$) (Figure 3A and B).
213 In contrast, there were no significant differences between genotypes in other brain nuclei (Figure 3A).
214 Similarly, expression of *gal* in the pPMp of *cyp19a1b*$^{-/-}$ males was reduced to 43% as compared with
215 *cyp19a1b*$^{+/+}$ males ($P = 0.0019$), while no significant differences were observed in other brain nuclei
216 (Figure 3C and D). These results demonstrate that *cyp19a1b* deficiency severely impairs the AR-
217 dependent activation of behaviorally relevant *vt* and *gal* expression, suggesting that brain-derived
218 estrogens play a substantial role in activating AR signaling.
219

220 **Estrogens directly stimulate the transcription of ARs through ESRs**

221 The above results led us to further explore how brain-derived estrogens stimulate the expression of
222 *ara* and *arb*. In silico analysis of the medaka *ara* and *arb* loci identified two canonical bipartite estrogen-
223 responsive element (ERE)-like sequences in introns 1 and 2 of *ara* (located at positions +1699 and
224 +2050, respectively, relative to the transcription initiation site) and three in the 5′-flanking region of *arb*
225 (at positions –1272, –2180, and –3327) (Figure 4A and B). Thus, brain estrogens might be able to
226 directly activate the transcription of *ara* and *arb*. To evaluate this likelihood, we conducted in vitro
227 transcriptional activity assays in which luciferase expression was driven by genomic fragments from the
228 *ara* and *arb* loci containing the identified ERE-like sequences.

229 An assay using the *ara* genomic fragment revealed that E2 dose-dependently increased luciferase
230 activity in the presence of any ESR subtype (Esr1, Esr2a, or Esr2b) (Figure 4C), suggesting that E2 has
231 the ability to directly activate *ara* transcription through ESRs. The introduction of a point mutation into
232 the ERE-like sequence at position +2050 abolished the E2-induced luciferase activity in the presence of

233 any ESR subtype, while mutation at +1699 had no such effect (Figure 4D). These results suggest that
234 the ERE at position +2050 is responsible for E2-induced activation of *ara* transcription. Because there
235 is evidence that a single ERE half-site is sufficient to confer E2 responsiveness on several genes (Klinge,
236 2001), we performed the assay using *ara* genomic fragments in which a mutation was introduced in
237 either half-site of the ERE at +2050. E2 induction of luciferase activity was abrogated in both cases
238 (Figure 4—figure supplement 1A), suggesting that both ERE half-sites are required to confer estrogen
239 responsiveness on *ara*.
240 In the assay using the *arb* genomic fragment, E2 also dose-dependently increased luciferase activity
241 in the presence of any ESR subtype (Figure 4E). The E2-induced increase was completely abolished by
242 point mutation of the ERE-like sequence at position –3327 in the presence of any ESR subtype (Figure
243 4F). A similar effect was observed for mutation of the ERE-like sequence at position –1272, but only in
244 the presence of Esr1 and not in the presence of Esr2a or Esr2b (Figure 4F). These results indicate that
245 E2 can directly stimulate *arb* transcription, primarily through the ERE at –3327. Mutations in either
246 half-site of this ERE eliminated induction by E2 in the presence of Esr2a or Esr2b, but not Esr1 (Figure
247 4—figure supplement 1B), suggesting that both ERE half-sites are required to confer estrogen
248 responsiveness on *arb*. Collectively, these experiments suggest that the transcription of *ara* and *arb* can
249 be directly stimulated by estrogens (including brain-derived estrogens) via the binding of ESRs to
250 canonical bipartite EREs.
251
252 **Brain-derived estrogens stimulate *ara* and *arb* expression in behaviorally relevant**
253 **brain regions primarily through Esr2a and Esr1, respectively**
254 Next, we investigated whether brain-derived estrogens can induce *ara* and *arb* expression through
255 ESRs in vivo and, if so, which ESR subtype (Esr1, Esr2a, or Esr2b) mediates this induction. To this end,
256 we examined *ara* and *arb* expression in the brains of males deficient for each ESR subtype by in situ
257 hybridization. We used previously described *esr1*- and *esr2b*-deficient medaka (Nishiike et al., 2021;
258 Fleming et al., 2023) and generated *esr2a*-deficient medaka using the CRISPR (clustered regularly
259 interspaced short palindromic repeats) / Cas9 (CRISPR-associated protein 9) system. Two independent
260 *esr2a*-deficient lines (Δ8 and Δ4) were established (Figure 5—figure supplement 1) and used for
261 subsequent behavioral experiments to ensure the reproducibility of the observed phenotypes.
262 In $esr1^{+/+}$ and $esr1^{-/-}$ males, *ara* expression was not significantly different between genotypes in any
263 brain nucleus (Figure 5—figure supplement 2A), but *arb* expression was significantly lower in $esr1^{-/-}$
264 than in $esr1^{+/+}$ males in the PMp and aPPp ($P = 0.0111$ and 0.0376, respectively) (Figure 5A and B). This,
265 together with our observation that *arb* expression in these brain nuclei was also significantly lower in
266 $cyp19a1b^{-/-}$ males (Figure 2H), suggests that brain-derived estrogens stimulate *arb* expression in these
267 nuclei primarily through Esr1. In support of this notion, double-label in situ hybridization in the wild-
268 type male brain detected neurons coexpressing *arb* and *esr1* in both the PMp and aPPp (Figure 5—figure
269 supplement 2B). In $esr2a^{+/+}$ and $esr2a^{-/-}$ male brains (from the Δ8 line), *ara* expression was significantly
270 lower in $esr2a^{-/-}$ than in $esr2a^{+/+}$ males in the PPa, pPPp, and NVT ($P = 0.0359$, 0.0430, and 0.0178,

respectively) (Figure 5C and D), while no significant difference was observed in *arb* expression (Figure 5—figure supplement 2C). Considering that *ara* expression in these nuclei was also lower in *cyp19a1b*$^{-/-}$ males (Figure 2F), brain-derived estrogens presumably stimulate *ara* expression in these nuclei mainly through Esr2a. This idea was further supported by double-label in situ hybridization, which detected neurons coexpressing *ara* and *esr2a* in the PPa, pPPp, and NVT of wild-type males (Figure 5—figure supplement 2D). Examination of *esr2b*$^{+/+}$ and *esr2b*$^{-/-}$ male brains showed significantly lower expression of *ara* in the NAT and higher expression of *arb* in the PPa of *esr2b*$^{-/-}$ males (Figure 5—figure supplement 2E–H); however, no such changes in expression were observed in *cyp19a1b*$^{-/-}$ males (Figure 2F and H). It therefore seems unlikely that Esr2b mediates the effect of brain estrogens on AR expression. Collectively, these results suggest that brain-derived estrogens stimulate *ara* and *arb* expression in behaviorally relevant brain regions primarily through Esr2a and Esr1, respectively.

esr1- and *esr2a*-deficient males are, respectively, less motivated to mate and less aggressive

If Esr1 and Esr2a truly mediate the behavioral effects of brain-derived estrogens through the activation of AR expression, then *esr1*- and *esr2a*-deficient males should exhibit impaired male-typical behaviors. More specifically, given that Esr1 and Esr2a function to activate the expression of *arb* and *ara*, which are responsible for male mating and aggression, respectively (Nishiike and Okubo, 2024), *esr1*- and *esr2a*-deficient males should be less motivated to mate and less aggressive, respectively.

To test these ideas, we first evaluated the mating behavior of *esr1*-deficient males using a wild-type female as the stimulus. As expected, *esr1*$^{-/-}$ males showed a significantly longer latency to initiate followings than *esr1*$^{+/+}$ males (P = 0.0055) (Figure 5—figure supplement 3), suggesting that they are less motivated to mate. This was further confirmed in tests using an *esr2b*-deficient female as the stimulus, where *esr1*$^{-/-}$ males showed a longer latency to followings and fewer courtship displays than *esr1*$^{+/+}$ males (P = 0.0426 and 0.0039, respectively) (Figure 5E–G). In contrast, no deficits were observed in the mating behavior of *esr2a*$^{-/-}$ males toward wild-type females (Figure 5—figure supplement 4A and B). Although *esr2a*$^{-/-}$ males of the Δ8 line showed a shorter latency to followings than their wild-type siblings in tests using a stimulus *esr2b*-deficient female (P = 0.0146) (Figure 5H–J), this was not reproduced in the Δ4 line (Figure 5—figure supplement 4C and D). We subsequently assessed aggressive behavior and found no defects in *esr1*$^{-/-}$ males (Figure 5K). Conversely, *esr2a*$^{-/-}$ males from both the Δ8 and Δ4 lines exhibited significantly fewer fin displays than their wild-type siblings (P = 0.0461 and 0.0293, respectively). Circles followed a similar pattern, with a significant reduction in the Δ8 line (P = 0.0446) and a comparable but non-significant decrease in the Δ4 line (P = 0.1512) (Figure 5L, Figure 5—figure supplement 3E), showing less aggression. Taken together with the previous finding that *esr2b*-deficient males show no deficits in either mating or aggressive behavior (Nishiike et al., 2021), these results suggest that brain-derived estrogens can promote mating with females by stimulating *arb* expression through Esr1 and can increase aggression toward other males by stimulating *ara* expression through Esr2a. Nonetheless, behavioral deficits in *esr1*- and *esr2a*-deficient

309 males were relatively mild as compared with *cyp19a1b*-deficient males (Figure 1) and *ara*- and *arb*-
310 deficient males (Nishiike and Okubo, 2024), suggesting that a compensatory mechanism may exist
311 between ESR subtypes.

Discussion

In this study, we found that male medaka deficient for *cyp19a1b* exhibit severely impaired male-typical mating and aggression. This observation was noteworthy because the fish had markedly elevated brain levels of 11KT, the primary driver of male-typical behaviors in teleosts (Okubo et al., 2022; Kawabata-Sakata et al., 2024). Deficits in mating were rescued by estrogen administration, indicating that reduced brain estrogen levels are the primary cause of the observed mating impairment; in other words, brain-derived estrogens are pivotal at least for male-typical mating behaviors in teleosts. This was also notable because, unlike in rodents, where the necessity for brain-derived estrogens has been codified as the "aromatization hypothesis", these estrogens have been regarded as dispensable for male behaviors in many vertebrates, including teleosts (Thornton et al., 2009; Bakker, 2022; Okubo et al., 2022). In addition, the rescue of behavioral phenotypes by estrogen administration in adults suggests that in teleosts, unlike in rodents, brain-derived estrogens early in life are not essential for the execution of male-typical behaviors. While brain-derived estrogens are necessary for male behaviors in both rodents and teleosts, the life stages at which they exert their behavioral effects probably differ between these species. Brain aromatase activity in teleosts increases with age and, at adulthood, reaches 100–1000 times that in rodents (Diotel et al., 2018; Okubo et al., 2022). In contrast, brain aromatase activity in rodents reaches its peak during the perinatal period and thereafter declines with age (Lephart, 1996), although it remains important for male behavior in adulthood. This variation among species may represent the activation of brain estrogen synthesis at life stages critical for sexual differentiation of behavior that are unique to each species.

Brain-derived estrogens serve several functions during the process of sexual differentiation of the mouse brain, including the synthesis of prostaglandin PGE2 and the activation of synaptic and neurodevelopmental genes; however, the specific mechanism whereby these estrogens affect male behaviors remains obscure (McCarthy et al., 2017; Gegenhuber et al., 2022; McCarthy, 2023). Our findings in medaka indicate that brain-derived estrogens facilitate male-typical behaviors by potentiating androgen/AR signaling in behaviorally relevant brain regions via the direct stimulation of AR transcription. More specifically, they indicate that brain-derived estrogens (1) promote mating by stimulating the transcription of *arb* in some preoptic and hypothalamus nuclei via Esr1, and (2) increase aggression by stimulating the transcription of *ara* in other preoptic and hypothalamus nuclei through Esr2a. This model of the mechanism underlying the action of brain-derived estrogens would explain the apparent contradiction that, in teleosts, androgens per se elicit male behaviors without aromatization, while estrogen synthesis in the brain are also critical for these behaviors. Our data also indicate that the two AR genes, *ara* and *arb*, are direct downstream targets of brain-derived estrogens that mediate male behaviors, only a few of which have been identified thus far. In mice, perinatal brain estrogens increase *Ar* expression in the bed nucleus of the stria terminalis and preoptic area, two brain regions that have been implicated in male behaviors (Juntti et al., 2010). Recent evidence suggests that ESR1 binds to the regulatory genomic region of *Ar* in these brain regions in mice (Gegenhuber et al., 2022). Given these

350 facts, the idea that brain-derived estrogens enhance androgen/AR signaling by directly stimulating AR
351 transcription may apply to a wide range of species, including rodents.
352 Consistent with our results, studies in several teleost species have shown that treatment of males
353 with an aromatase inhibitor reduces their male-typical behaviors, while estrogens exert the opposite
354 effect (Hallgren et al., 2006; O'Connell and Hofmann, 2012; Huffman et al., 2013; Jalabert et al., 2015).
355 Conversely, it has been shown in various teleosts, including medaka, that treatment with exogenous
356 estrogens attenuates male behaviors (Bayley et al., 1999; Bell, 2001; Bjerselius et al., 2001; Oshima et
357 al., 2003; Martinović et al., 2007). A possible explanation for this discrepancy is that estrogens may
358 either stimulate or suppress male-typical behaviors, depending on their concentration. All studies
359 showing the suppressive effects of exogenous estrogens were conducted at doses higher than those used
360 in the present study or at doses mimicking the levels typical of adult females (Kayo et al., 2020). In
361 addition, our previous study in male medaka showed that high doses of exogenous estrogens induce the
362 expression of *esr2b*, which prevents male-typical mating behavior, in behaviorally relevant brain regions
363 (Nishiike et al., 2021). Thus, the development of male behaviors may require moderate brain estrogen
364 levels that are sufficient to induce the expression of *ara* and *arb*, but not *esr2b*, in the underlying neural
365 circuitry. Considering this, the lack of aggression recovery in E2-treated *cyp19a1b*-deficient males in
366 this study may be explained by the possibility that the E2 dose used was sufficient to induce not only
367 *ara* and *arb* but also *esr2b* expression in aggression-relevant circuits, which potentially suppressed
368 aggression. Another possibility that is not mutually exclusive is that endogenous levels of brain
369 estrogens are sufficient to motivate males to engage in male-typical behaviors, and therefore exogenous
370 estrogens have no further effect. This possibility is at least likely for mating behavior, as estrogen
371 treatment facilitated mating behavior in *cyp19a1b*-deficient males but not in their wild-type siblings.
372 Further studies using *cyp19a1b* mutants from different teleost species are needed to explore these
373 possibilities and to determine whether the findings in medaka hold for other teleosts.
374 In summary, we have shown that brain-derived estrogens promote male-typical behaviors by
375 increasing brain sensitivity to testicular androgens through the stimulation of AR expression. Our
376 findings challenge the prevailing view that brain-derived estrogens have little effect on male-typical
377 behaviors in species where testicular androgens elicit these behaviors directly without aromatization to
378 estrogens in the brain and unveil a previously unappreciated mechanism of the action of brain-derived
379 estrogens. Because these species account for the majority of vertebrates, with rodents and some birds
380 being the only known exceptions, the mechanism of their action that we have identified in medaka may
381 be evolutionarily ancient and widely conserved across species.

382 # Materials and methods

383

384 ## Animals and cell lines

385 Wild-type d-rR strain medaka and mutant medaka deficient for *cyp19a1b* and *esr2a* (generated in
386 this study), *esr1* (Fleming et al., 2023), and *esr2b* (Nishiike et al., 2021) were maintained in a
387 recirculating system at 28ºC on a 14/10-hour light/dark cycle. Three or four times a day, they were fed
388 live brine shrimp and dry food (Otohime; Marubeni Nisshin Feed, Tokyo, Japan). Sexually mature adults
389 (2–6 months) were used for experiments and assigned randomly to experimental groups. Tissues were
390 consistently sampled 1–5 hours after lights on. In each experiment, siblings raised under the same
391 conditions were used as the comparison group to control for the effects of genetic diversity and
392 environmental variation.

393 HEK293T and HeLa cells used in this study were confirmed to be mycoplasma-free (Biotherapy
394 Institute of Japan, Tokyo, Japan) and authenticated by short tandem repeat profiling (National Institute
395 of Biomedical Innovation, Osaka, Japan).

396

397 ## Generation of mutant medaka

398 *cyp19a1b*-deficient medaka were generated essentially as previously described (Nishiike et al.,
399 2021). In brief, a TILLING library of 5760 chemically mutagenized medaka (Taniguchi et al., 2006)
400 was screened for mutations in exons 3, 4, and 5 of *cyp19a1b* by direct sequencing of PCR-amplified
401 fragments. A founder (ID: 57D05) with a nonsense mutation in exon 4 (K105*) was identified (Figure
402 1—figure supplement 1A and B) and backcrossed to the wild-type d-rR strain for more than six
403 generations to eliminate background mutations. Heterozygous males and females were intercrossed to
404 generate wild-type, heterozygous, and homozygous siblings. All experimental fish were subjected to
405 genotyping by PCR amplification across the mutation, followed by high-resolution melting (HRM)
406 analysis, using the primers and probe listed in Supplementary file 2. HRM analysis was performed on
407 the LightCycler 480 System II (Roche Diagnostics, Basel, Switzerland) using the LCGreen Plus dye
408 (BioFire Defense, Salt Lake City, UT).

409 *esr2a*-deficient medaka were generated by using the CRISPR/Cas9 system. A CRISPR RNA
410 (crRNA) targeting exon 3 of *esr2a* (Fasmac, Kanagawa, Japan) (Figure 5—figure supplement 1A) was
411 injected with trans-activating crRNA (Fasmac) and Cas9 protein (Nippon Gene Co. Ltd., Tokyo, Japan)
412 into the cytoplasm of one- or two-cell stage embryos. The resulting fish were screened for germline
413 mutations by outcrossing to wild-type fish and testing progeny for target site mutations by T7
414 endonuclease I assay (Kim et al., 2009) and direct sequencing. Two founders were identified that
415 reproducibly yielded progeny carrying frameshift mutations that eliminated the DNA- and ligand-
416 binding domains of Esr2a: one yielded progeny carrying an 8-bp deletion (Δ8); the other yielded progeny
417 carrying a 4-bp deletion (Δ4) (Figure 5—figure supplement 1A and B). The DNA- and ligand-binding
418 domains of medaka Esr2a were identified by sequence alignment with yellow perch (*Perca flavescens*)
419 Esr2a, for which these domain locations have been reported (Lynn et al., 2008). The progeny were

420 intercrossed to obtain wild-type, heterozygous, and homozygous siblings. The genotype of each
421 experimental fish was determined by HRM analysis as described above.
422 A previous study reported that *esr2a*-deficient female medaka cannot release eggs due to oviduct
423 atresia (Kayo et al., 2019). Likewise, some *esr2a*-deficient females generated in this study, despite the
424 limited sample size, exhibited spawning behavior but were unable to release eggs (Δ8 line: 2/3; Δ4 line:
425 1/1), while such failure was not observed in wild-type females (Δ8 line: 0/12; Δ4 line: 0/11). These
426 results support the effective loss of *esr2a* function.
427
428 **Measurement of sex steroid levels**
429 Brain and peripheral levels of sex steroids were determined by enzyme-linked immunosorbent assay
430 (ELISA) (Nishiike et al., 2021). Total lipids were extracted from the brain and from peripheral tissues,
431 specifically the caudal half of the body excluding the head and visceral organs, of *cyp19a1b*$^{+/+}$,
432 *cyp19a1b*$^{+/-}$, and *cyp19a1b*$^{-/-}$ males with chloroform/methanol (2:1, v/v) and purified on a Sep-Pak C18
433 Plus Light Cartridge (Waters Corporation, Milford, MA). Tissue levels of E2, testosterone, and 11KT
434 were measured by using Estradiol, Testosterone, and 11-Keto Testosterone ELISA kits, respectively
435 (Cayman Chemical Company, Ann Arbor, MI).
436
437 **Real-time PCR**
438 Total RNA was isolated from the brains of *cyp19a1b*$^{+/+}$, *cyp19a1b*$^{+/-}$, and *cyp19a1b*$^{-/-}$ males using
439 the RNeasy Plus Universal Mini Kit (Qiagen, Hilden, Germany). cDNA was synthesized with the
440 SuperScript VILO cDNA Synthesis Kit (Thermo Fisher Scientific, Waltham, MA). Real-time PCR was
441 performed on the LightCycler 480 System II using the LightCycler 480 SYBR Green I Master (Roche
442 Diagnostics). Melting curve analysis was conducted to verify that a single amplicon was obtained in
443 each sample. The β-actin gene (*actb*; GenBank accession number NM_001104808) was used to
444 normalize the levels of target transcripts. The primers used for real-time PCR are shown in
445 Supplementary file 2.
446
447 **Protein structure prediction**
448 Structural predictions of Cyp19a1b proteins were conducted using AlphaFold 3 (Abramson et al.,
449 2024). Amino acid sequences corresponding to the wild-type allele and the mutant allele generated in
450 this study were submitted to the AlphaFold 3 prediction server. The resulting models were visualized
451 with PyMOL (Schrödinger, New York, NY), and key structural features, including the membrane helix,
452 aromatic region, and heme-binding loop, were annotated.
453
454 **Mating behavior test**
455 Mating behavior was tested essentially as previously described (Hiraki-Kajiyama et al., 2019). In
456 brief, on the day before behavioral testing, each focal male (*cyp19a1b*-, *esr1*-, and *esr2a*-deficient lines)
457 was placed with a stimulus female (wild-type females in the tests shown in Figure 1D and E, Figure 5—

figure supplement 3, and Figure 5—figure supplement 4A and B; *esr2b*-deficient females in Figure 1F–I, Figure 2A–E, Figure 5E–J, and Figure 5—figure supplement 4C and D) in a 2-liter rectangular tank with a perforated transparent partition separating them. The set-up was modified for E2-treated males, which were kept on E2 treatment and not introduced to the test tanks until the day of testing to ensure the efficacy of E2 treatment. The partition was removed 1 hour after lights on, and fish were allowed to interact for 30 min while their behavior was recorded with a digital video camera (HC-V360MS, HC-VX985M, or HC-W870M; Panasonic Corporation, Osaka, Japan). The first 15 min of the recording was used to calculate the latency to the first following, courtship display, wrapping, and spawning. In tests using an *esr2b*-deficient female as the stimulus fish, the latency to spawn could not be calculated because the female was unreceptive to males and did not spawn. Therefore, the sexual motivation of the focal male was assessed by counting the number of courtship displays and wrapping attempts in 30 min. To evaluate courtship displays performed by stimulus *esr2b*-deficient females toward focal males, the recording period was extended to 2 hours, as these females take longer to initiate courtship (Nishiike et al., 2021). In all video analyses, the researcher was blind to the fish genotype and treatment.

Aggressive behavior test

To test male–male aggressive behavior (Yamashita et al., 2020), four males of the same genotype (*cyp19a1b*-, *esr1*-, and *esr2a*-deficient lines) that were unfamiliar with one another were placed together in a test tank 1 hour after lights on. After 1 min of acclimation to the tank, fish were allowed to interact for 15 min while their behavior was video-recorded as described above. The total number of each aggressive act (chase, fin display, circle, strike, and bite) displayed by the four males in the tank was counted manually from the video recordings.

E2 treatment

cyp19a1b$^{+/+}$ and *cyp19a1b*$^{-/-}$ males were treated with 1 ng/ml of E2 (Fujifilm Wako Pure Chemical, Osaka, Japan), which was first dissolved in 100% ethanol (vehicle), or with the vehicle alone by immersion in water for 4 days, with daily water changes to maintain the nominal concentration. The mating and aggressive behaviors of males before and after E2 treatment were evaluated as described above. The expression of *ara* and *arb* in the brain of E2- and vehicle-treated males was investigated by single-label in situ hybridization as described below. Although the exact increase in brain E2 levels following E2 treatment was not quantified, the observed positive effects on behavior and gene expression suggest that it was sufficient.

Single-label in situ hybridization

Digoxigenin (DIG)-labeled cRNA probes were generated by in vitro transcription using DIG RNA Labeling Mix (Roche Diagnostics), T7 RNA polymerase (Roche Diagnostics), and the following cDNA fragments: *ara*, nucleotide 16–1030 of GenBank NM_001122911 (1015 bp); *arb*, 53–1233 of NM_001104681 (1181 bp); *vt*, 1–845 of NM_001278891 (845 bp); and *gal*, 5–533 of LC532140 (529

496 bp).

497 Single-label in situ hybridization was essentially done as described (Kawabata-Sakata et al., 2020).
498 In brief, male brains from the *cyp19a1b*-deficient line (analysis of *ara*, *arb*, *vt*, and *gal*) and from the
499 *esr1*-, *esr2a*-, and *esr2b*-deficient lines (analysis of *ara* and *arb*) were fixed in 4% paraformaldehyde
500 and embedded in paraffin. Serial coronal sections of 10-μm thickness were hybridized with a DIG-
501 labeled probe. Hybridization signal was detected with anti-DIG conjugated to alkaline phosphatase
502 (RRID: AB_514497; Roche Diagnostics) and visualized using 5-bromo-4-chloro-3-indolyl
503 phosphate/nitro blue tetrazolium substrate (Roche Diagnostics). After color development for 15 min
504 (*gal*), 2 hours (*vt*), or overnight (*ara* and *arb*), sections were imaged using a VS120 virtual slide
505 microscope (Olympus, Tokyo, Japan). The total area of signal across all relevant sections, including
506 both hemispheres, was calculated for each brain nucleus using Olyvia software (Olympus). Images were
507 converted to a 256-level intensity scale, and pixels with intensities from 161 to 256 were considered
508 signals. All sections used for comparison were processed in the same batch, without corrections between
509 samples. Medaka brain atlases (Anken and Bourrat, 1998; Ishikawa et al., 1999) were used to identify
510 brain nuclei.

511

512 **Transcriptional activity assay**

513 Each full-length coding region of medaka Esr1 (GenBank XM_020714493), Esr2a
514 (NM_001104702), and Esr2b (XM_020713365) cDNA was amplified by PCR and inserted into the
515 expression vector pcDNA3.1/V5-His-TOPO (Thermo Fisher Scientific). Each nucleotide sequence of
516 the 5′-flanking region of *ara* and *arb* was retrieved from the Ensembl medaka genome assembly and
517 analyzed for potential canonical ERE-like sequences using Jaspar (version 5.0_alpha) and Match (public
518 version 1.0) with default settings. No ERE-like sequence was detected in *ara*; therefore, the gene body
519 and 3′-flanking region were also analyzed in this case. The transcription initiation site for *ara* and *arb*
520 was determined based on an expressed sequence tag clone deposited in National BioResource Project
521 (NBRP) Medaka (olova36n18) and GenBank NM_001104681, respectively. Medaka bacterial artificial
522 chromosome (BAC) clones containing the *ara* (clone ID: ola1-111G01) and *arb* (ola1-192H15) loci
523 were obtained from NBRP Medaka. A 4530-bp genomic DNA fragment upstream of *ara* exon 3
524 (comprising 2330 bp of the 5′-flanking region, exon 1, intron 1, exon 2, intron 2, and the first 32 bp of
525 exon 3) was amplified by PCR from the BAC clone, fused to a P2A self-cleaving peptide sequence (Kim
526 et al., 2011) at the 3′ end, and inserted into the NheI site of the luciferase reporter vector pGL4.10
527 (Promega, Madison, WI). Similarly, a 3995-bp fragment upstream of the first methionine codon of *arb*
528 (comprising 3815 bp of the 5′-flanking region and 180 bp of exon1) was PCR-amplified and inserted
529 into pGL4.10. The resulting constructs were transiently transfected into HEK293T (*ara*) or HeLa (*arb*)
530 cells, together with an internal control vector pGL4.74 (Promega) and the Esr1, Esr2a, or Esr2b
531 expression construct using Lipofectamine LTX (Thermo Fisher Scientific). Six hours after transfection,
532 cells were incubated for 18 hours without and with E2 at doses of 10^{-11} M, 10^{-9} M, and 10^{-7} M in
533 Dulbecco's modified Eagle's medium (phenol red-free) containing 5% charcoal/dextran-stripped fetal

534 bovine serum (Cytiva, Marlborough, MA). Luciferase activity was determined using the Dual-
535 Luciferase Reporter Assay System (Promega) on the GloMax 20/20n Luminometer (Promega). All
536 assays were conducted in duplicate or triplicate and repeated independently three times.
537 Further assays were performed with luciferase reporter constructs carrying point mutations in the
538 ERE-like sequences to identify the ERE responsible for E2 induction of *ara* and *arb* transcription. Each
539 half-site of the responsible ERE-like sequence was mutated into a HindIII recognition site using the
540 PrimeSTAR Mutagenesis Basal Kit (Takara Bio, Shiga, Japan). Transcriptional activity assays with
541 these constructs were done as described above, except that a single dose of E2 (10^{-7} M) was used.
542

543 **Double-label in situ hybridization**

544 DIG-labeled cRNA probes for *ara* and *arb* were prepared as described above. Fluorescein-labeled
545 cRNA probes for *esr1* and *esr2a* were generated by in vitro transcription using Fluorescein RNA
546 Labeling Mix (Roche Diagnostics), SP6 or T7 RNA polymerase (Roche Diagnostics), and the following
547 cDNA fragments: *esr1*, nucleotides 1694–2781 of XM_020714493 (1088 bp); *esr2a*, 1838–2276 of
548 NM_001104702 plus 763 bp of 3′-untranslated sequence derived from the Ensembl medaka genome
549 assembly (439 bp).
550 Double-label in situ hybridization was done as described previously (Fleming et al., 2023), with
551 minor modifications. In brief, brains dissected from wild-type males were fixed in 4% paraformaldehyde,
552 embedded in paraffin, and coronally sectioned at 10-µm thickness. Sections were hybridized
553 simultaneously with the DIG-labeled *ara* or *arb* probe and fluorescein-labeled *esr1* or *esr2a* probe. DIG
554 was detected with a mouse anti-DIG antibody (RRID: AB_304362; Abcam, Cambridge, UK) and
555 visualized using the Alexa Fluor 555 Tyramide SuperBoost Kit, goat anti-mouse IgG (Thermo Fisher
556 Scientific); fluorescein was detected with an anti-fluorescein antibody conjugated to horseradish
557 peroxidase (RRID: AB_2737388; PerkinElmer, Waltham, MA) and visualized using the TSA Plus
558 Fluorescein System (PerkinElmer). Cell nuclei were counterstained with DAPI. Fluorescent images
559 were acquired with a Leica TCS SP8 confocal laser scanning microscope (Leica Microsystems, Wetzlar,
560 Germany) and the following excitation/emission wavelengths: 552/620–700 nm (Alexa Fluor 555),
561 488/495–545 nm (fluorescein), and 405/410–480 nm (DAPI). Cells were identified as coexpressing the
562 two genes when Alexa Fluor 555 and fluorescein signals were clearly observed in the cytoplasm
563 surrounding DAPI-stained nuclei, with intensities markedly stronger than the background noise.
564

565 **Statistical analysis**

566 All quantitative data were expressed as mean ± standard error of the mean (SEM). On graphs,
567 individual data points were plotted to indicate the underlying distribution. Behavioral time-series data
568 were analyzed using Kaplan–Meier plots with the inclusion of fish that did not exhibit the given act
569 within the test period.
570 Statistical analyses were done using GraphPad Prism (GraphPad Software, San Diego, CA). Data
571 between two groups were compared using unpaired two-tailed Student's *t* test. Welch's correction was

572 applied if the *F* test indicated that the variance between groups was significantly different. The
573 Bonferroni–Dunn correction was applied for multiple comparisons between two groups. To compare
574 data among more than two groups, one-way analysis of variance (ANOVA) was performed, followed
575 by either Bonferroni's (comparisons among experimental groups) or Dunnett's (comparisons between
576 untreated and E2-treated groups in Figure 4C and D) post hoc test. If the Brown-Forsythe test indicated
577 a significant difference in variance across groups, the data were instead analyzed using the non-
578 parametric Kruskal–Wallis test, followed by Dunn's post hoc test. Differences between Kaplan–Meier
579 curves were tested for significance using the Gehan–Breslow–Wilcoxon test (with Bonferroni's
580 correction for more than two comparisons). Fish that spawned without any courtship display were
581 excluded from the analysis of courtship display because it was not appropriate to treat them either as
582 fish that did not perform courtship displays within the test duration or as fish that performed the first
583 courtship display 0 seconds before spawning. Specifically, 7/18 *cyp19a1b*$^{+/+}$, 11/18 *cyp19a1b*$^{+/-}$, and
584 6/18 *cyp19a1b*$^{-/-}$ males were excluded in Figure 1E; 2/23 *esr1*$^{+/+}$ and 5/24 *esr1*$^{-/-}$ males were excluded
585 in Figure 5—figure supplement 3; 2/24 *esr2a*$^{+/+}$ and 3/23 *esr2a*$^{-/-}$ males were excluded in Figure 5—
586 figure supplement 4A; 0/23 *esr2a*$^{+/+}$ and 0/23 *esr2a*$^{-/-}$ males were excluded in Figure 5—figure
587 supplement 4B. All data points were included in the analyses and no outliers were defined.
588 No power analysis was conducted due to the lack of relevant data; sample size was estimated based
589 on previous studies reporting inter-individual variation in behavior and neural gene expression in
590 medaka.

Acknowledgments

We thank NBRP Medaka for providing the BAC clones, managing the TILLING library, and performing artificial insemination; Dr. Yoshihito Taniguchi for constructing the TILLING library; Dr. Masatoshi Nakamoto for recovering the *cyp19a1b* mutant allele; Akira Hirata, Kaoru Furukawa, Tomiko Iba, and Ayu Kuwakubo for assistance with medaka husbandry.

References

1. Abramson J, Adler J, Dunger J, Evans R, Green T, Pritzel A, Ronneberger O, Willmore L, Ballard AJ, Bambrick J, Bodenstein SW, Evans DA, Hung CC, O'Neill M, Reiman D, Tunyasuvunakool K, Wu Z, Žemgulytė A, Arvaniti E, Beattie C, Bertolli O, Bridgland A, Cherepanov A, Congreve M, Cowen-Rivers AI, Cowie A, Figurnov M, Fuchs FB, Gladman H, Jain R, Khan YA, Low CMR, Perlin K, Potapenko A, Savy P, Singh S, Stecula A, Thillaisundaram A, Tong C, Yakneen S, Zhong ED, Zielinski M, Žídek A, Bapst V, Kohli P, Jaderberg M, Hassabis D, Jumper JM. 2024. Accurate structure prediction of biomolecular interactions with AlphaFold 3. *Nature* **630**:493–500. DOI: https://doi.org/10.1038/s41586-024-07487-w
2. Alward BA, Laud VA, Skalnik CJ, York RA, Juntti SA, Fernald RD. 2020. Modular genetic control of social status in a cichlid fish. *Proceedings of the National Academy of Sciences of the United States of America* **117**:28167–28174. DOI: https://doi.org/10.1073/pnas.2008925117
3. Anken R, Bourrat F. 1998. *Brain Atlas of the Medaka fish*. INRA Editions. ISBN13: 9782738008183
4. Bakker J. 2022. The role of steroid hormones in the sexual differentiation of the human brain. *Journal of Neuroendocrinology* **34**:e13050. DOI: https://doi.org/10.1111/jne.13050
5. Balthazart J. 2019. New concepts in the study of the sexual differentiation and activation of reproductive behavior, a personal view. *Frontiers in Neuroendocrinology* **55**:100785. DOI: https://doi.org/10.1016/j.yfrne.2019.100785
6. Bayley M, Nielsen JR, Baatrup E. 1999. Guppy sexual behavior as an effect biomarker of estrogen mimics. *Ecotoxicology and Environmental Safety* **43**:68–73. DOI: https://doi.org/10.1006/eesa.1999.1766
7. Bell AM. 2001. Effects of an endocrine disrupter on courtship and aggressive behaviour of male three-spined stickleback, *Gasterosteus aculeatus*. *Animal Behaviour* **62**:775–780. DOI: https://doi.org/10.1006/anbe.2001.1824
8. Bjerselius R, Lundstedt-Enkel K, Olsén H, Mayer I, Dimberg K. 2001. Male goldfish reproductive behaviour and physiology are severely affected by exogenous exposure to 17β-estradiol. *Aquatic Toxicology* **53**:139–152. DOI: https://doi.org/10.1016/s0166-445x(00)00160-0
9. Diotel N, Charlier TD, Lefebvre d'Hellencourt C, Couret D, Trudeau VL, Nicolau JC, Meilhac O, Kah O, Pellegrini E. 2018. Steroid transport, local synthesis, and signaling within the brain: roles in neurogenesis, neuroprotection, and sexual behaviors. *Frontiers in Neuroscience* **12**:84. DOI: https://doi.org/10.3389/fnins.2018.00084
10. Diotel N, Le Page Y, Mouriec K, Tong SK, Pellegrini E, Vaillant C, Anglade I, Brion F, Pakdel F, Chung BC, Kah O. 2010. Aromatase in the brain of teleost fish: expression, regulation and putative functions. *Frontiers in Neuroendocrinology* **31**:172–192. DOI: https://doi.org/10.1016/j.yfrne.2010.01.003
11. Fleming T, Tachizawa M, Nishiike Y, Koiwa A, Homan Y, Okubo K. 2023. Estrogen-dependent

635 expression and function of secretogranin 2a in female-specific peptidergic neurons. *PNAS Nexus*
636 **2**:pgad413. DOI: https://doi.org/10.1093/pnasnexus/pgad413
637 12. Forlano PM, Deitcher DL, Myers DA, Bass AH. 2001. Anatomical distribution and cellular basis
638 for high levels of aromatase activity in the brain of teleost fish: aromatase enzyme and mRNA
639 expression identify glia as source. *The Journal of Neuroscience* **21**:8943–8955. DOI:
640 https://doi.org/10.1523/JNEUROSCI.21-22-08943.2001
641 13. Gegenhuber B, Wu MV, Bronstein R, Tollkuhn J. 2022. Gene regulation by gonadal hormone
642 receptors underlies brain sex differences. *Nature* **606**:153–159. DOI:
643 https://doi.org/10.1038/s41586-022-04686-1
644 14. Hallgren SL, Linderoth M, Olsén KH. 2006. Inhibition of cytochrome p450 brain aromatase
645 reduces two male specific sexual behaviours in the male Endler guppy (*Poecilia reticulata*).
646 *General and Comparative Endocrinology* **147**:323–328. DOI:
647 https://doi.org/10.1016/j.ygcen.2006.02.005
648 15. Hiraki T, Takeuchi A, Tsumaki T, Zempo B, Kanda S, Oka Y, Nagahama Y, Okubo K. 2012.
649 Female-specific target sites for both oestrogen and androgen in the teleost brain. *Proceedings of*
650 *the Royal Society B: Biological Sciences* **279**:5014–5023. DOI:
651 https://doi.org/10.1098/rspb.2012.2011
652 16. Hiraki-Kajiyama T, Yamashita J, Yokoyama K, Kikuchi Y, Nakajo M, Miyazoe D, Nishiike Y,
653 Ishikawa K, Hosono K, Kawabata-Sakata Y, Ansai S, Kinoshita M, Nagahama Y, Okubo K. 2019.
654 Neuropeptide B mediates female sexual receptivity in medaka fish, acting in a female-specific but
655 reversible manner. *eLife* **8**:e39495. DOI: https://doi.org/10.7554/eLife.39495
656 17. Huffman LS, O'Connell LA, Hofmann HA. 2013. Aromatase regulates aggression in the African
657 cichlid fish *Astatotilapia burtoni*. *Physiology & Behavior* **112**:77–83. DOI:
658 https://doi.org/10.1016/j.physbeh.2013.02.004
659 18. Ishikawa Y, Yoshimoto M, Ito H. 1999. A brain atlas of a wild-type inbred strain of the medaka,
660 *Oryzias latipes*. *The fish biology journal Medaka* **10**:1–26. DOI:
661 https://doi.org/10.18999/fisbjm.10.1
662 19. Jalabert C, Quintana L, Pessina P, Silva A. 2015. Extra-gonadal steroids modulate non-breeding
663 territorial aggression in weakly electric fish. *Hormones and Behavior* **72**:60–67. DOI:
664 https://doi.org/10.1016/j.yhbeh.2015.05.003
665 20. Juntti SA, Tollkuhn J, Wu MV, Fraser EJ, Soderborg T, Tan S, Honda S, Harada N, Shah NM. 2010.
666 The androgen receptor governs the execution, but not programming, of male sexual and territorial
667 behaviors. *Neuron* **66**:260–272. DOI: https://doi.org/10.1016/j.neuron.2010.03.024
668 21. Kawabata Y, Hiraki T, Takeuchi A, Okubo K. 2012. Sex differences in the expression of
669 vasotocin/isotocin, gonadotropin-releasing hormone, and tyrosine and tryptophan hydroxylase
670 family genes in the medaka brain. *Neuroscience* **218**:65–77. DOI:
671 https://doi.org/10.1016/j.neuroscience.2012.05.021
672 22. Kawabata-Sakata Y, Kanda S, Okubo K. 2024. Male-specific vasotocin expression in the medaka

tuberal hypothalamus: androgen dependence and probable role in aggression. *Molecular and Cellular Endocrinology* **580**:112101. DOI: https://doi.org/10.1016/j.mce.2023.112101

23. Kawabata-Sakata Y, Nishiike Y, Fleming T, Kikuchi Y, Okubo K. 2020. Androgen-dependent sexual dimorphism in pituitary tryptophan hydroxylase expression: relevance to sex differences in pituitary hormones. *Proceedings of the Royal Society B: Biological Sciences* **287**, 20200713. DOI: https://doi.org/10.1098/rspb.2020.0713
24. Kayo D, Oka Y, Kanda S. 2020. Examination of methods for manipulating serum 17β-Estradiol (E2) levels by analysis of blood E2 concentration in medaka (*Oryzias latipes*). *General and Comparative Endocrinology* **285**:113272. DOI: https://doi.org/10.1016/j.ygcen.2019.113272
25. Kayo D, Zempo B, Tomihara S, Oka Y, Kanda S. 2019. Gene knockout analysis reveals essentiality of estrogen receptor β1 (Esr2a) for female reproduction in medaka. *Scientific Reports* **9**:8868. DOI: https://doi.org/10.1038/s41598-019-45373-y
26. Kim HJ, Lee HJ, Kim H, Cho SW, Kim JS. 2009. Targeted genome editing in human cells with zinc finger nucleases constructed via modular assembly. *Genome Research* **19**:1279–1288. DOI: https://doi.org/10.1101/gr.089417.108
27. Kim JH, Lee SR, Li LH, Park HJ, Park JH, Lee KY, Kim MK, Shin BA, Choi SY. 2011. High cleavage efficiency of a 2A peptide derived from porcine teschovirus-1 in human cell lines, zebrafish and mice. *PLoS One* **6**:e18556. DOI: https://doi.org/10.1371/journal.pone.0018556
28. Klinge CM. 2001. Estrogen receptor interaction with estrogen response elements. *Nucleic Acids Research* **29**:2905–2919. DOI: https://doi.org/10.1093/nar/29.14.2905
29. Lephart ED. 1996. A review of brain aromatase cytochrome P450. *Brain Research Reviews* **22**:1–26. DOI: https://doi.org/10.1016/0165-0173(96)00002-1
30. Lindeboom RGH, Vermeulen M, Lehner B, Supek F. 2019. The impact of nonsense-mediated mRNA decay on genetic disease, gene editing and cancer immunotherapy. *Nature Genetics* **51**:1645–1651. DOI: https://doi.org/10.1038/s41588-019-0517-5
31. Lynn SG, Birge WJ, Shepherd BS. 2008. Molecular characterization and sex-specific tissue expression of estrogen receptor α (*esr1*), estrogen receptor βa (*esr2a*) and ovarian aromatase (*cyp19a1a*) in yellow perch (*Perca flavescens*). *Comparative Biochemistry and Physiology Part B: Biochemistry & Molecular Biology* **149**:126–147. DOI: https://doi.org/10.1016/j.cbpb.2007.09.001
32. Martinović D, Hogarth WT, Jones RE, Sorensen PW. 2007. Environmental estrogens suppress hormones, behavior, and reproductive fitness in male fathead minnows. *Environmental Toxicology and Chemistry* **26**:271–278. DOI: https://doi.org/10.1897/06-065r.1
33. McCarthy MM. 2023. Neural control of sexually dimorphic social behavior: connecting development to adulthood. *The Annual Review of Neuroscience* **46**:321–339. DOI: https://doi.org/10.1146/annurev-neuro-121522-110856
34. McCarthy MM, Nugent BM, Lenz KM. 2017. Neuroimmunology and neuroepigenetics in the establishment of sex differences in the brain. *Nature Reviews Neuroscience* **18**:471–484. DOI: https://doi.org/10.1038/nrn.2017.61

35. Nagahama Y, Chakraborty T, Paul-Prasanth B, Ohta K, Nakamura M. 2021. Sex determination, gonadal sex differentiation, and plasticity in vertebrate species. *Physiological Reviews* **101**:1237–1308. DOI: https://doi.org/10.1152/physrev.00044.2019
36. Nakamoto M, Shibata Y, Ohno K, Usami T, Kamei Y, Taniguchi Y, Todo T, Sakamoto T, Young G, Swanson P, Naruse K, Nagahama Y. 2018. Ovarian aromatase loss-of-function mutant medaka undergo ovary degeneration and partial female-to-male sex reversal after puberty. *Molecular and Cellular Endocrinology* **460**:104–122. DOI: https://doi.org/10.1016/j.mce.2017.07.013
37. Nishiike Y, Miyazoe D, Togawa R, Yokoyama K, Nakasone K, Miyata M, Kikuchi Y, Kamei Y, Todo T, Ishikawa-Fujiwara T, Ohno K, Usami T, Nagahama Y, Okubo K. 2021. Estrogen receptor 2b is the major determinant of sex-typical mating behavior and sexual preference in medaka. *Current Biology* **31**:1699–1710.e6. DOI: https://doi.org/10.1016/j.cub.2021.01.089
38. Nishiike Y, Okubo K. 2024. The decision of male medaka to mate or fight depends on two complementary androgen signaling pathways. *Proceedings of the National Academy of Sciences of the United States of America* **121**:e2316459121. DOI: https://doi.org/10.1073/pnas.2316459121
39. O'Connell LA, Hofmann HA. 2012. Social status predicts how sex steroid receptors regulate complex behavior across levels of biological organization. *Endocrinology* **153**:1341–1351. DOI: https://doi.org/10.1210/en.2011-1663
40. Ogawa S, Tsukahara S, Choleris E, Vasudevan N. 2020. Estrogenic regulation of social behavior and sexually dimorphic brain formation. *Neuroscience & Biobehavioral Reviews* **110**:46–59. DOI: https://doi.org/10.1016/j.neubiorev.2018.10.012
41. Ogino Y, Ansai S, Watanabe E, Yasugi M, Katayama Y, Sakamoto H, Okamoto K, Okubo K, Yamamoto Y, Hara I, Yamazaki T, Kato A, Kamei Y, Naruse K, Ohta K, Ogino H, Sakamoto T, Miyagawa S, Sato T, Yamada G, Baker ME, Iguchi T. 2023. Evolutionary differentiation of androgen receptor is responsible for sexual characteristic development in a teleost fish. *Nature Communications* **14**:1428. DOI: https://doi.org/10.1038/s41467-023-37026-6
42. Okubo K, Nishiike Y, Fleming T, Kikuchi Y, Hiraki-Kajiyama T. 2022. "Sex steroid regulation of male- and female-typical mating behaviors in teleost fish" in *Spectrum of Sex*, Tanaka M, Tachibana M Eds. Springer Nature. pp.111–133. DOI: https://doi.org/10.1007/978-981-19-5359-0_7
43. Okubo K, Takeuchi A, Chaube R, Paul-Prasanth B, Kanda S, Oka Y, Nagahama Y. 2011. Sex differences in aromatase gene expression in the medaka brain. *Journal of Neuroendocrinology* **23**:412–423. DOI: https://doi.org/10.1111/j.1365-2826.2011.02120.x
44. Oshima Y, Kang IJ, Kobayashi M, Nakayama K, Imada N, Honjo T. 2003. Suppression of sexual behavior in male Japanese medaka (*Oryzias latipes*) exposed to 17β-estradiol. *Chemosphere* **50**:429–436. DOI: https://doi.org/10.1016/s0045-6535(02)00494-0
45. Takeuchi A, Okubo K. 2013. Post-proliferative immature radial glial cells female-specifically express aromatase in the medaka optic tectum. *PLoS One* **8**:e73663. DOI: https://doi.org/10.1371/journal.pone.0073663
46. Taniguchi Y, Takeda S, Furutani-Seiki M, Kamei Y, Todo T, Sasado T, Deguchi T, Kondoh H,

Mudde J, Yamazoe M, Hidaka M, Mitani H, Toyoda A, Sakaki Y, Plasterk RH, Cuppen E. 2006. Generation of medaka gene knockout models by target-selected mutagenesis. *Genome Biology* **7**:R116. DOI: https://doi.org/10.1186/gb-2006-7-12-r116

47. Terasawa E. 2018. Neuroestradiol in regulation of GnRH release. *Hormones and Behavior* **104**:138–145. DOI: https://doi.org/10.1016/j.yhbeh.2018.04.003
48. Thornton J, Zehr JL, Loose MD. 2009. Effects of prenatal androgens on rhesus monkeys: a model system to explore the organizational hypothesis in primates. *Hormones and Behavior* **55**:633–645. DOI: https://doi.org/10.1016/j.yhbeh.2009.03.015
49. Tripp JA, Salas-Allende I, Makowski A, Bass AH. 2020. Mating behavioral function of preoptic galanin neurons is shared between fish with alternative male reproductive tactics and tetrapods. *The Journal of Neuroscience* **40**:1549–1559. DOI: https://doi.org/10.1523/JNEUROSCI.1276-19.2019
50. Tsukahara S, Morishita M. 2020. Sexually dimorphic formation of the preoptic area and the bed nucleus of the stria terminalis by neuroestrogens. *Frontiers in Neuroscience* **14**:797. DOI: https://doi.org/10.3389/fnins.2020.00797
51. Yamanaka O, Takeuchi R. 2018. UMATracker: an intuitive image-based tracking platform. *Journal of Experimental Biology* **221**:jeb182469. DOI: https://doi.org/10.1242/jeb.182469
52. Yamashita J, Takeuchi A, Hosono K, Fleming T, Nagahama Y, Okubo K. 2020. Male-predominant galanin mediates androgen-dependent aggressive chases in medaka. *eLife* **9**:e59470. DOI: https://doi.org/10.7554/eLife.59470
53. Yokoi S, Okuyama T, Kamei Y, Naruse K, Taniguchi Y, Ansai S, Kinoshita M, Young LJ, Takemori N, Kubo T, Takeuchi H. 2015. An essential role of the arginine vasotocin system in mate-guarding behaviors in triadic relationships of medaka fish (*Oryzias latipes*). *PLoS Genetics* **11**:e1005009. DOI: https://doi.org/10.1371/journal.pgen.1005009
54. Yong L, Thet Z, Zhu Y. 2017. Genetic editing of the androgen receptor contributes to impaired male courtship behavior in zebrafish. *Journal of Experimental Biology* **220**:3017–3021. DOI: https://doi.org/10.1242/jeb.161596
55. Zhang X, Min Q, Li M, Liu X, Li M, Wang D. 2019. Mutation of *cyp19a1b* results in sterile males due to efferent duct obstruction in Nile tilapia. *Molecular Reproduction and Development* **86**:1224–1235. DOI: https://doi.org/10.1002/mrd.23237
56. Zilkha N, Sofer Y, Kashash Y, Kimchi T. 2021. The social network: neural control of sex differences in reproductive behaviors, motivation, and response to social isolation. *Current Opinion in Neurobiology* **68**:137–151. DOI: https://doi.org/10.1016/j.conb.2021.03.005

Figure legends

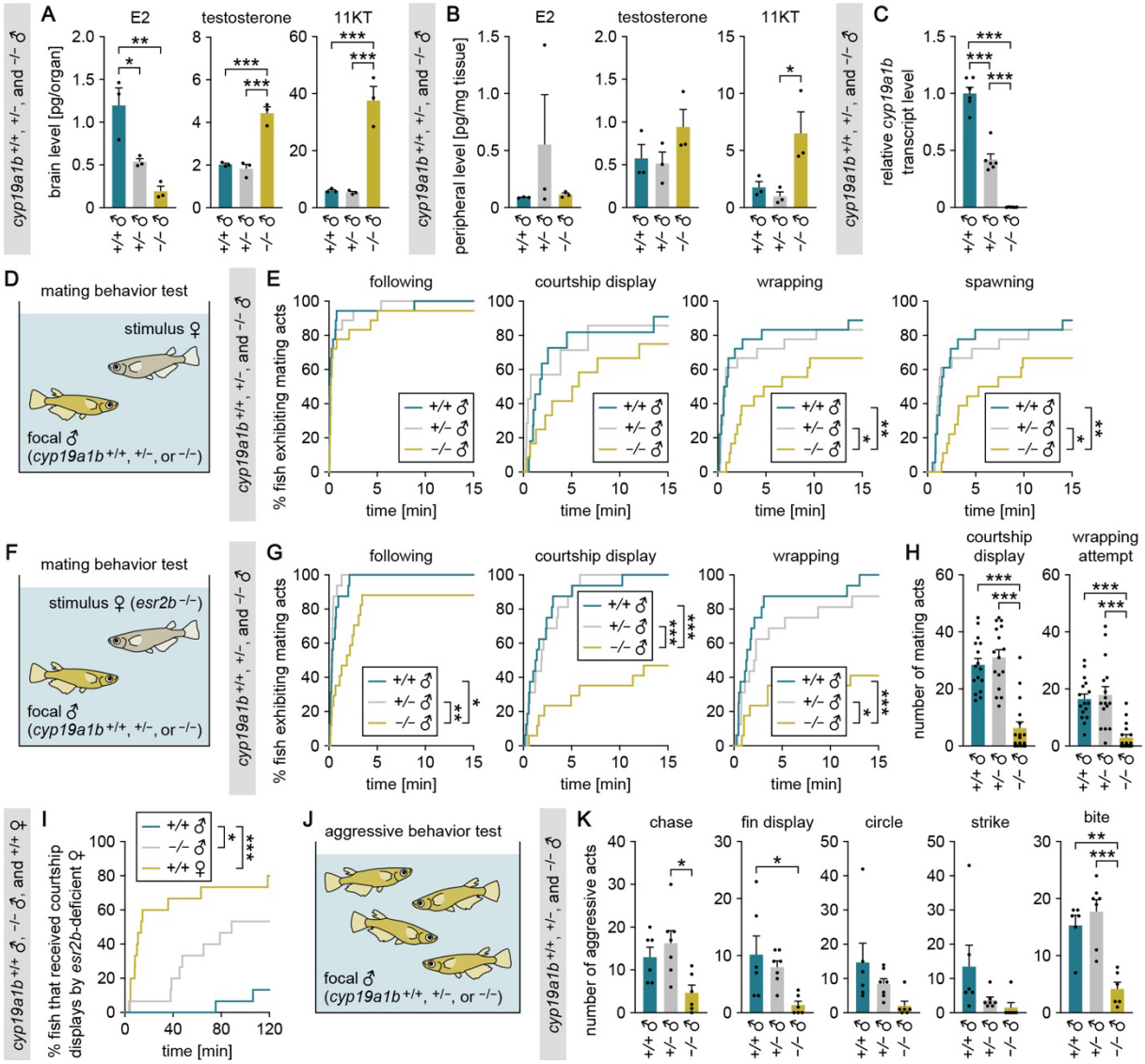

Figure 1. *cyp19a1b*-deficient males exhibit severely impaired male-typical mating and aggressive behaviors.

(**A**, **B**) Levels of E2, testosterone, and 11KT in the brain (A) and periphery (B) of adult *cyp19a1b*$^{+/+}$, *cyp19a1b*$^{+/-}$, and *cyp19a1b*$^{-/-}$ males (n = 3 per genotype). (**C**) Brain *cyp19a1b* transcript levels in *cyp19a1b*$^{+/+}$, *cyp19a1b*$^{+/-}$, and *cyp19a1b*$^{-/-}$ males (n = 6 per genotype). Mean value for *cyp19a1b*$^{+/+}$ males was arbitrarily set to 1. (**D**) Set-up for testing the mating behavior of *cyp19a1b*$^{+/+}$, *cyp19a1b*$^{+/-}$, and *cyp19a1b*$^{-/-}$ males. (**E**) Latency of *cyp19a1b*$^{+/+}$, *cyp19a1b*$^{+/-}$, and *cyp19a1b*$^{-/-}$ males (n = 18 per genotype) to initiate each mating act toward the stimulus female. (**F**) Set-up for testing mating behavior using an *esr2b*-deficient female as the stimulus. (**G**) Latency of *cyp19a1b*$^{+/+}$, *cyp19a1b*$^{+/-}$, and *cyp19a1b*$^{-/-}$ males (n = 16, 15, and 17, respectively) to initiate each mating act toward the *esr2b*-deficient female. (**H**) Number of each mating act performed. (**I**) Latency of *cyp19a1b*$^{+/+}$ and *cyp19a1b*$^{-/-}$ males and *cyp19a1b*$^{+/+}$ females (n = 15 each) to receive courtship displays from the *esr2b*-deficient

798 female. (**J**) Set-up for testing aggressive behavior among grouped males. (**K**) Total number of each
799 aggressive act performed by *cyp19a1b*$^{+/+}$, *cyp19a1b*$^{+/-}$, and *cyp19a1b*$^{-/-}$ males. Each data point
800 represents the sum of acts recorded for the 4 males of the same genotype in a single tank (n = 6, 7, and
801 5 tanks, respectively). Statistical differences were assessed by Bonferroni's or Dunn's post hoc test (A,
802 B, C, H, K) and Gehan-Breslow-Wilcoxon test with Bonferroni's correction (E, G, I). Error bars
803 represent SEM. *$P < 0.05$, **$P < 0.01$, ***$P < 0.001$.

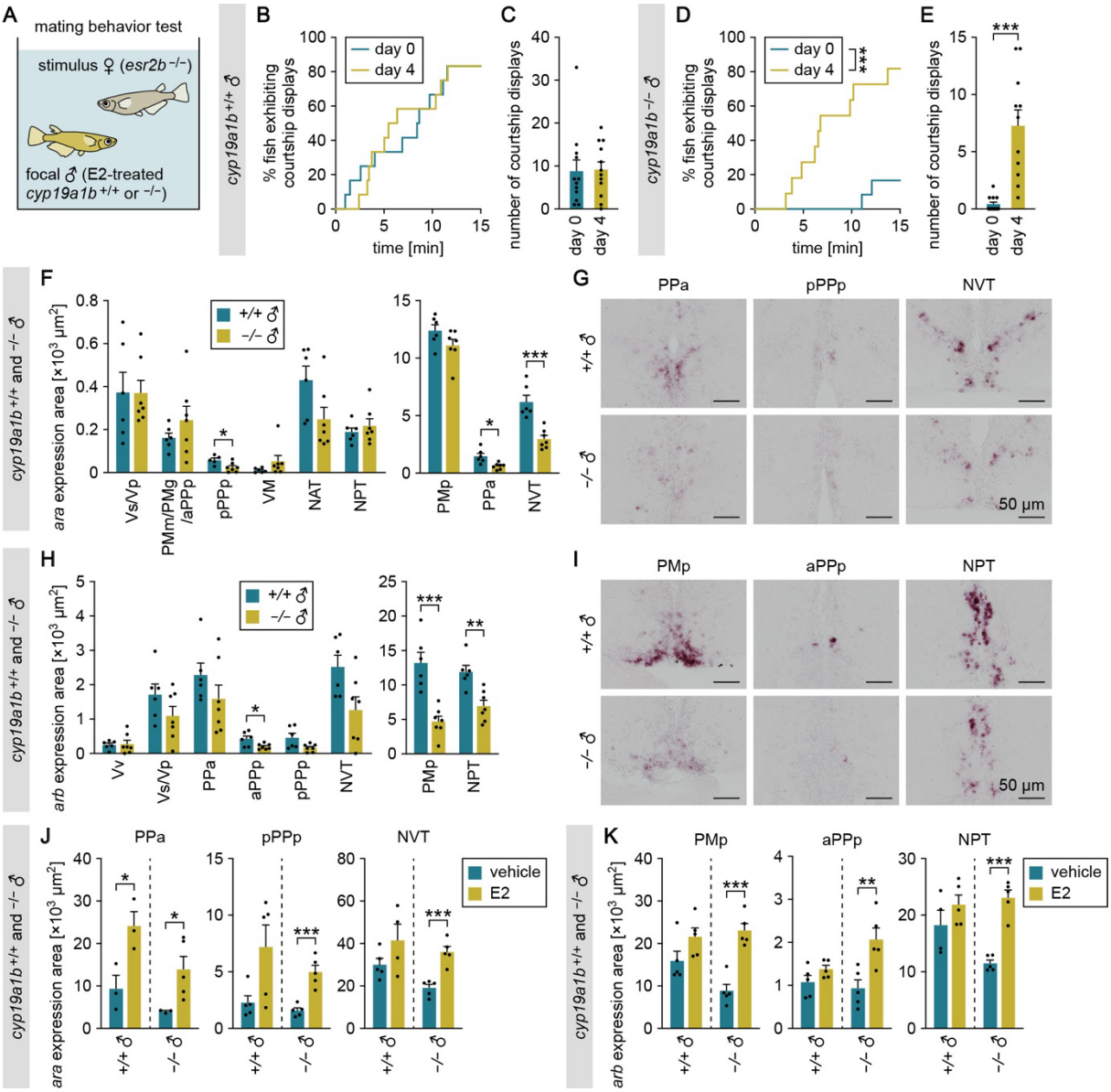

Figure 2. Brain-derived estrogens facilitate male-typical behaviors probably by stimulating brain AR expression.

(**A**) Set-up for testing the mating behavior of E2-treated *cyp19a1b*$^{+/+}$ and *cyp19a1b*$^{-/-}$ males. (**B**) Latency of *cyp19a1b*$^{+/+}$ males (n = 12) to initiate courtship displays toward the stimulus female before (day 0) and after (day 4) E2 treatment. (**C**) Number of courtship displays performed by *cyp19a1b*$^{+/+}$ males. (**D**) Latency of *cyp19a1b*$^{-/-}$ males (n = 12) to initiate courtship displays before (day 0) and after (day 4) E2 treatment. (**E**) Number of courtship displays performed by *cyp19a1b*$^{-/-}$ males. (**F**) Total area of *ara* expression signal in each brain nucleus of *cyp19a1b*$^{+/+}$ (n = 6 except for pPPp, where n = 5) and *cyp19a1b*$^{-/-}$ (n = 7) males. The data are displayed in two graphs for visual clarity. (**G**) Representative images of *ara* expression in the PPa, pPPp, and NVT. (**H**) Total area of *arb* expression signal in each brain nucleus of *cyp19a1b*$^{+/+}$ (n = 6) and *cyp19a1b*$^{-/-}$ (n = 7 except for NVT, where n = 6) males. The data are displayed in two graphs for visual clarity. (**I**) Representative images of *arb* expression in the PMp, aPPp, and NPT. (**J**) Total area of *ara* expression signal in the PPa, pPPp, and NVT of *cyp19a1b*$^{+/+}$

819 and *cyp19a1b*$^{-/-}$ males treated with vehicle alone or E2 (n = 5 per group except for NVT of E2-treated
820 *cyp19a1b*$^{+/+}$ males, where n = 4; and PPa of vehicle-treated *cyp19a1b*$^{+/+}$, E2-treated *cyp19a1b*$^{+/+}$, and
821 vehicle-treated *cyp19a1b*$^{-/-}$ males, where n = 3). (**K**) Total area of *arb* expression signal in the PMp,
822 aPPp, and NPT of *cyp19a1b*$^{+/+}$ and *cyp19a1b*$^{-/-}$ males treated with vehicle alone or E2 (n = 5 per group
823 except for NPT of vehicle-treated *cyp19a1b*$^{+/+}$ males, where n = 4). Scale bars represent 50 μm. For
824 abbreviations of brain nuclei, see Supplementary file 1. Statistical differences were assessed by Gehan-
825 Breslow-Wilcoxon test (B, D) and unpaired *t* test, with Welch's correction where appropriate (C, E, F,
826 H, J, K). Error bars represent SEM. *$P < 0.05$, **$P < 0.01$, ***$P < 0.001$.

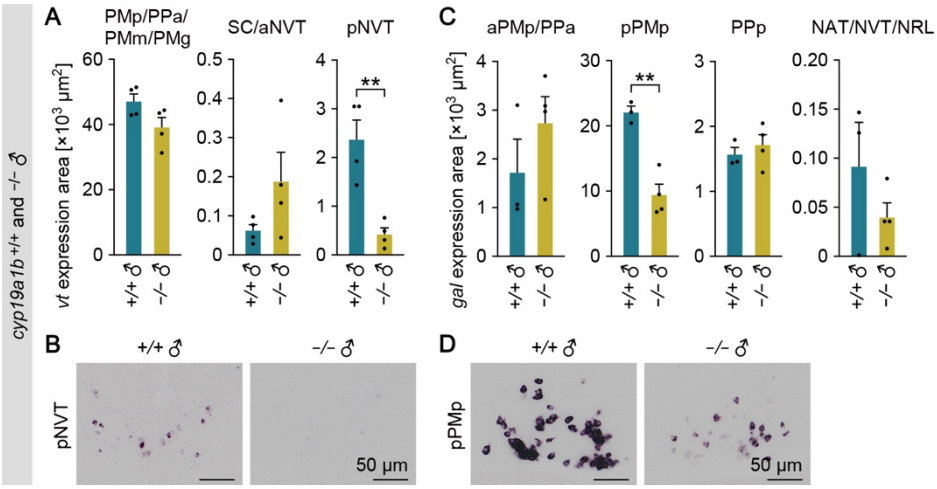

827
828

829 **Figure 3. *cyp19a1b* deficiency impairs behaviorally relevant signaling pathways**
830 **downstream of ARs.**

831 (**A**) Total area of *vt* expression signal in the PMp/PPa/PMm/PMg, SC/aNVT, and pNVT of *cyp19a1b*$^{+/+}$
832 and *cyp19a1b*$^{-/-}$ males (n = 4 per genotype). (**B**) Representative images of *vt* expression in the pNVT.
833 (**C**) Total area of *gal* expression signal in the aPMp/PPa, pPMp, PPp, and NAT/NVT/NRL of
834 *cyp19a1b*$^{+/+}$ and *cyp19a1b*$^{-/-}$ males (n = 3 and 4, respectively). (**D**) Representative images of *gal*
835 expression in the pPMp. Scale bars represent 50 µm. For abbreviations of brain nuclei, see
836 Supplementary file 1. Statistical differences were assessed by unpaired *t* test, with Welch's correction
837 where appropriate (A, C). Error bars represent SEM. $^{**}P < 0.01$.

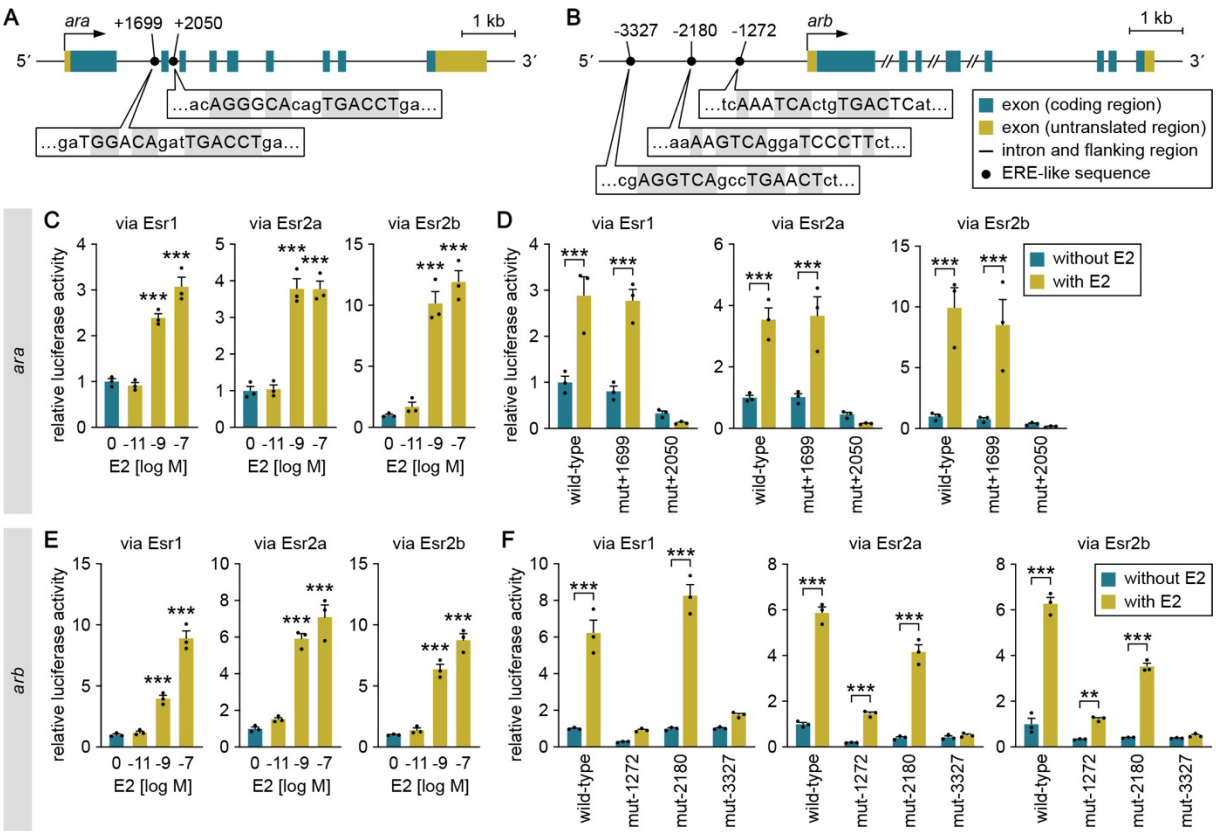

Figure 4. Estrogens directly stimulate the transcription of ARs through ESRs.

(**A**, **B**) Schematic of *ara* (A) and *arb* (B) loci showing the location of the canonical bipartite ERE-like sequences. Bent arrows mark the transcription initiation sites. Nucleotides of the ERE-like sequences are denoted by capital letters, and those identical to the consensus ERE (AGGTCAnnnTGACCT) are gray-shaded. (**C**) Ability of E2 to directly activate *ara* transcription. Cultured cells were transfected with a luciferase reporter construct containing a genomic fragment upstream of exon 3 of *ara*, together with an Esr1, Esr2a, or Esr2b expression construct. The cells were stimulated with different concentrations of E2 and luciferase activity was measured. (**D**) Effect of mutations in the ERE-like sequences on the E2-induced activation of *ara* transcription. Cultured cells were transfected with a wild-type luciferase construct or a construct carrying a mutation in the ERE-like sequence at position +1699 (mut+1699) or +2050 (mut+2050), together with an Esr1, Esr2a, or Esr2b expression construct. The cells were stimulated with or without E2, and luciferase activity was measured. (**E**) Ability of E2 to directly activate *arb* transcription. The assay described in C was performed with a luciferase construct containing a genomic fragment upstream of the first methionine codon of *arb*. (**F**) Effect of mutations in the ERE-like sequences on the E2-induced activation of *arb* transcription. The assay described in D was performed with luciferase constructs each carrying a mutation in the ERE-like sequence at position –1272 (mut-1272), –2180 (mut-2180), or –3327 (mut-3327). Values are expressed as a fold change relative to a control without E2 stimulation (C, E) or a control using the wild-type construct without E2 stimulation (D, F). Statistical differences were assessed by Dunnett's post hoc test (C, E) and unpaired *t* test with Bonferroni–Dunn correction (D, F). Error bars represent SEM. $^{**}P < 0.01$; $^{***}P < 0.001$.

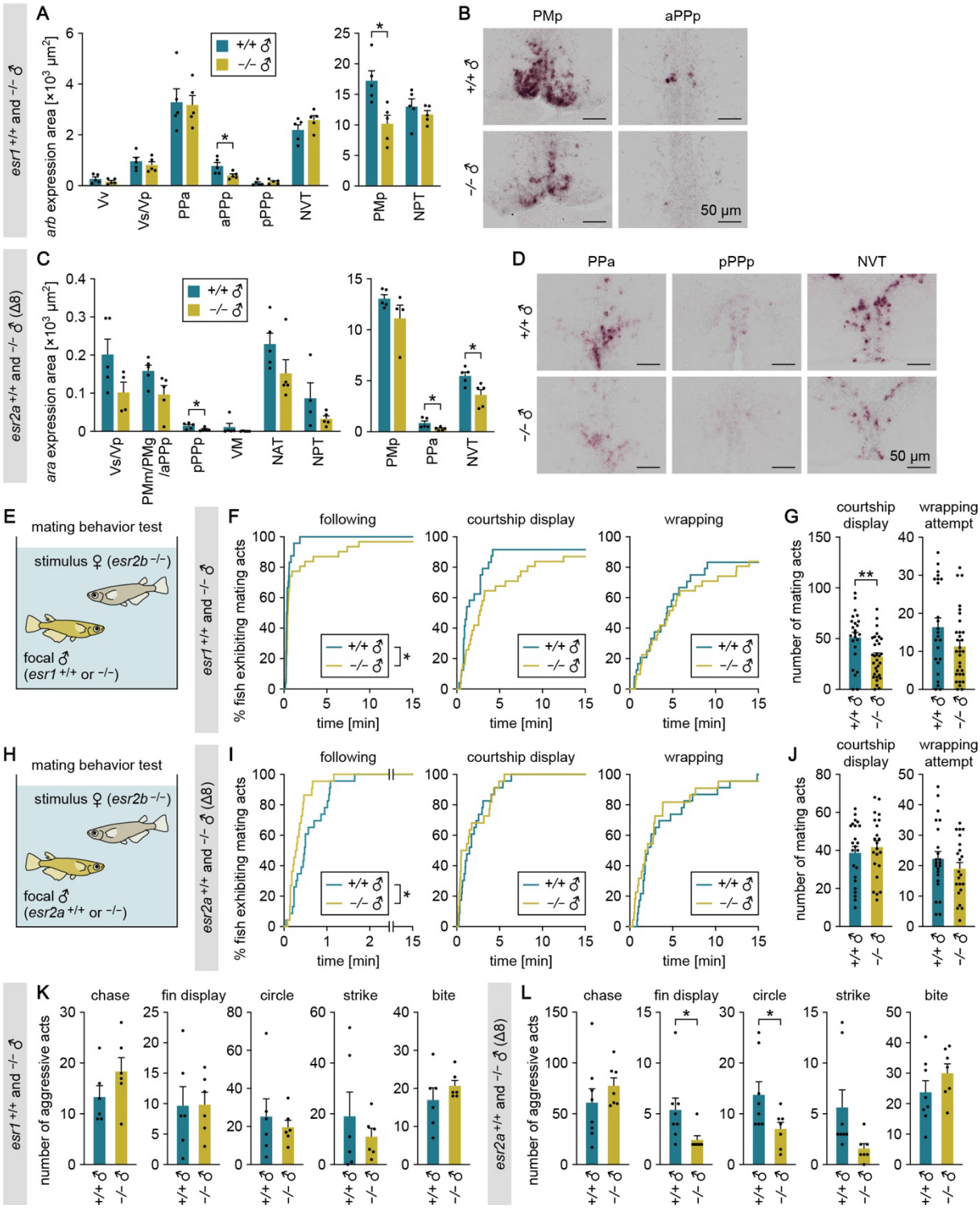

Figure 5. Brain-derived estrogens stimulate *ara* and *arb* expression in behaviorally relevant brain regions primarily through Esr2a and Esr1, respectively.

(**A**) Total area of *arb* expression signal in each brain nucleus of $esr1^{+/+}$ and $esr1^{-/-}$ males (n = 5 per genotype). The data are displayed in two graphs for visual clarity. (**B**) Representative images of *arb* expression in the PMp and aPPp. (**C**) Total area of *ara* expression signal in each brain nucleus of $esr2a^{+/+}$ and $esr2a^{-/-}$ males (Δ8 line; n = 5 per genotype except for NPT of $esr2a^{+/+}$ males and Vs/Vp and PMp

868 of *esr2a*$^{-/-}$ males, where n = 4). The data are displayed in two graphs for visual clarity. (**D**)
869 Representative images of *ara* expression in the PPa, pPPp, and NVT. (**E**) Set-up for testing the mating
870 behavior of *esr1*$^{+/+}$ and *esr1*$^{-/-}$ males using an *esr2b*-deficient female as the stimulus. (**F**) Latency of
871 *esr1*$^{+/+}$ and *esr1*$^{-/-}$ males (n = 24 and 31, respectively) to initiate each mating act toward the stimulus
872 female. (**G**) Number of each mating act performed. (**H**) Set-up for testing the mating behavior of *esr2a*$^{+/+}$
873 and *esr2a*$^{-/-}$ males using an *esr2b*-deficient female as the stimulus. (**I**) Latency of *esr2a*$^{+/+}$ and *esr2a*$^{-/-}$
874 males (Δ8 line; n = 23 and 22, respectively) to initiate each mating act toward the stimulus female. (**J**)
875 Number of each mating act performed. (**K**, **L**) Total number of each aggressive act observed among
876 *esr1*$^{+/+}$ or *esr1*$^{-/-}$ males (n = 6 per genotype) (K) and among *esr2a*$^{+/+}$ or *esr2a*$^{-/-}$ males (Δ8 line; n = 8
877 and 7, respectively) (L) in the tank. Scale bars represent 50 μm. For abbreviations of brain nuclei, see
878 Supplementary file 1. Statistical differences were assessed by unpaired *t* test, with Welch's correction
879 where appropriate (A, C, G, J, K, L) and Gehan-Breslow-Wilcoxon test (F, I). Error bars represent SEM.
880 *$P < 0.05$, **$P < 0.01$.